Turkish Journal of Engineering

https://dergipark.org.tr/en/pub/tuje

e-ISSN 2587-1366

Microstructural analysis of ZnO-CuPc nanocomposites synthenised by hydrothermal method

Rekawt Khdir Hamad [1], Canan Aksu Canbay [*1], İskender Özkul [2]

[1]Fırat University, Faculty of Science, Department of Physics, Elazığ, Turkey
[2]Mersin University, Engineering Faculty, Department of Mechanical Engineering, Mersin, Turkey

Keywords
Composite
Hydrothermal method
Structural characterization
EDX
XRD
SEM

ABSTRACT

With the discovery of inorganic semiconductors, silicon and germanium became very important materials in the field of electronics. The use of these materials with these limited features for a long time has become insufficient in the face of increasing demands. For this reason, organic semiconductors have revolutionized structures that respond to these demands. In this study, we synthesized ZnO based semi-material with the hydrothermal method. Structural characterizations were made by XRD, SEM (EDX) and FTIR.

1. INTRODUCTION

Semiconductor materials are frequently used in electronics field in the world. Thanks to this equipment used in different signal collector sensors in renewable energy applications, sectors such as computers and medical nuclear have made remarkable progress (Kahraman et al. 2014). Generally, inorganic semiconductor materials are used in these applications. Elements such as silicon or germanium play the main role in the formation of these components. However, the fact that the studies with these materials are close to the saturation level requires different searches. Organic materials are the best alternative for this situation and are accepted. In many electronic and optoelectronic applications, inorganic semiconductors (polymeric / non-polymeric) have started to take their place.

Hydrocarbons such as Anthracene and phthalocyanine may show semiconductor properties. The main feature of semiconductors is electrical conductivity, which depends on the mobility and concentration of charge carriers. Organic semiconductors' electrical conductivity, carrier concentrations, and mobility are lower than that of inorganic semiconductors. A comparison of the properties of an organic conductor, Copper phthalocyanine and inorganic semiconductor germanium is given in Table 1.

ZnO based composites attracted the attention of researchers (Güler et al. 2016; Güler et al. 2019). For this research study, our aim is to produce ZnO based composite materials in different compositions by hydrothermal method which is the new production method. Following the production, the structural and morphological properties of the obtained composite materials were investigated. These analyses were conducted with X-Ray Diffraction (XRD), scanning electron microscopy (SEM) and Fourier transform infrared (FTIR) analysis.

Table 1. Comparison of the electrical properties of the inorganic semiconductor germanium and organic semiconductor CuPc (Heilmeier and Warfield 1963; Xavier 1997)

Properties	Inorganic	Organic
Mobility (cm^2/ V. Sec)	3900	1
Carrier concentration (cm^{-3})	2.5×10^{13}	$10^6$to 10^7
Trap density (cm^{-3})	-	$10^{12}$to 10^{14}
Resistivity (ohm . cm)	43	10^{14}
Bandgap (eV)	0.67	1.6
Density (g/cm^3)	5.32	1.6

2. EXPERIMENTAL

In this work, Zinc acetate $Zn(CH3COO)_2$ and sodium hydroxide NaOH were used. Zinc acetate was dissolved in distilled water. Then, sodium hydroxide 0.85gm was dissolved in 20 ml distilled water, separately and stirring during 1h on the magnetic stirrer. After this, the two solutions put into the same cup, placed into hydrothermal equipment at 160 °C and stayed for 12 h. Then we open the hydrothermal system and the final solution was transferred to autoclave and heated

* **Corresponding Author**

(rekawtphysic@gmail.com) ORCID ID 0000 – 0003 – 3804 – 022X
*(caksu@firat.edu.tr) ORCID ID 0000 – 0002 – 5151 – 4576
(iskender@mersin.edu.tr) ORCID ID 0000 – 0003 – 4255 – 0564

Cite this article

Hamad R K, Canbay C A & Özkul İ (2021). Microstructural analysis of ZnO-CuPc nanocomposites synthenised by hydrothermal method. Turkish Journal of Engineering, 5(3), 105-110

Research Article / DOI: 10.31127/tuje.695630

Received: 27/02/2020; Accepted: 21/04/2020

material dried at 100°C for 24h. In this study, four different samples were produced, and details are given as below;

Sample 1: $ZnO_{0.01}$ Mix with 2ml C_6H_5Cl inside a cup,

Sample 2: $ZnO_{0.01}$ Mix with $CuPc_{0.001}$ and 2ml C_6H_5Cl inside a cup,

Sample 3: $ZnO_{0.01}$ Mix with $CuPc_{0.002}$ and 2ml C_6H_5Cl inside a cup,

Sample 4: $ZnO_{0.01}$ Mix with $CuPc_{0.003}$ and 2ml C_6H_5Cl inside the cup.

After the production of the samples, we made the XRD, FTIR, SEM and EDX analysis.

3. RESULTS AND DISCUSSION

3.1. X-ray Diffraction Analysis

The X-ray measurements of the samples were made at room temperature to determine the diffraction planes. The X-ray diffraction pattern of pure CuPc is given in Fig. 1 (Hussein et al. 2016).

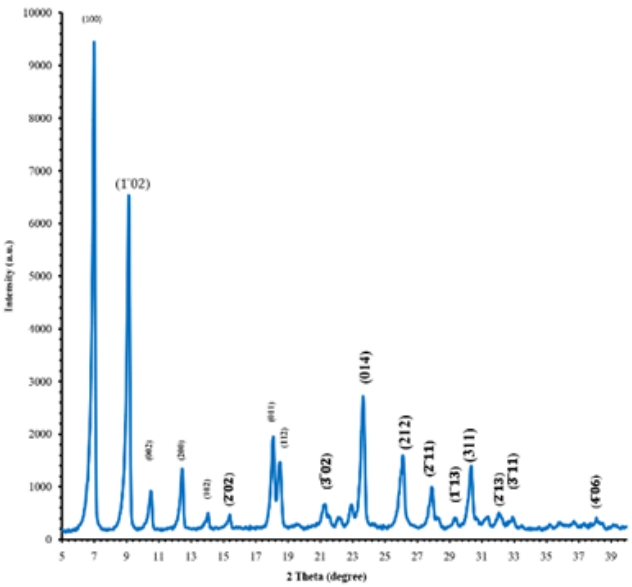

Figure 1. The XRD spectrum for CuPc powder

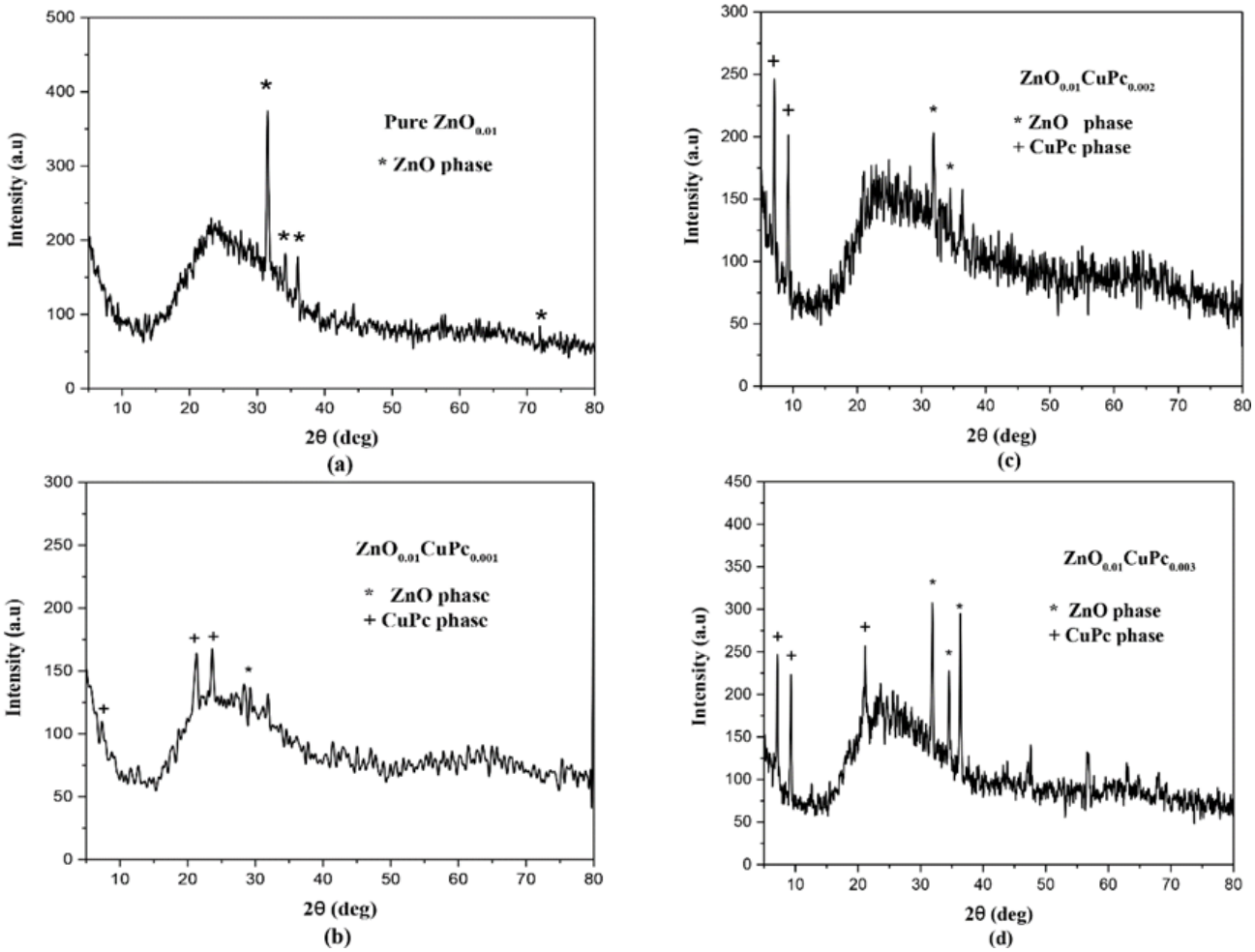

Figure 2. Diffraction pattern for (a) Pure ZnO, (b) $ZnO_{0.01}CuPc_{0.001}$, (c) $ZnO_{0.01}CuPc_{0.002}$, (d) $ZnO_{0.01}CuPc_{0.003}$

Fig.2 shows the X-ray diffraction patterns for ZnO-CuPc composite thin films deposited on a glass substrate. The prepared ZnO-CuPc nanocomposite diffraction pattern displays the hexagonal ZnO phase and for Cu-Pc has different crystal phases: α-, β- and χ– phases. All the peaks of the ZnO thin films correspond to the peaks of ZnO (JCPDS # 0.36- 1451). Peaks ZnO was signed by (*) and peaks CuPc was signed by (+).

The value of d-spacing, relative intensity and FWHM corresponding to Xray diffraction for all four samples have been tabulated in Table 3. It is found the value d-spacing by this equation.

$$n\lambda = 2d \sin\theta \quad (1)$$

The crystallites sizes (D) of the films are estimated using the Scherrer formula (Scherrer 1918).

$$D = \frac{K\lambda}{\beta COS(\theta)} \quad (2)$$

Where λ is the wavelength of X-Ray used (λ = 1.54 Å), k is shape factor constant taken to be 0.94, θ is diffracting angle and β is the full width at half maximum of peaks in XRD pattern. The value of crystallite size were given in Table 2.

The dislocation density (δ), defined as the length of dislocation lines per unit volume, is estimated using the following equation (Khan et al. 2010).

$$\delta = \frac{1}{D^2} \quad (3)$$

We found the dislocation density (δ) showed in Table 2.

The value of lattice Strain (ε) of the samples is estimated using the equation (Saleem *et al.* 2012).

$$\varepsilon = \frac{\beta \cos(\theta)}{4} \quad (4)$$

The calculated value of lattice Strain (ε) were given in Table 2.

Table 2. (2θ), d-spacing, FWHM, Crystallite size, strain and dislocation for ZnO-CuPc nanocomposite samples

Sample	(2θ)(°)	d(A°)	FWHM (°)	FWHM (rad)	The crystallite size (nm)	Strain (* 10^{-3})	Dislocation (*10^3)(nm)$^{-2}$
Pure $ZnO_{0.01}$	31.69	2.82	0.44	0.0076	19.45	1.86	2.64
$ZnO_{0.01}CuPc_{0.001}$	7.42	12.03	0.36	0.0062	23.6	1.54	1.79
$ZnO_{0.01}CuPc_{0.002}$	9.26	9.62	0.39	0.0068	21.49	1.69	2.16
$ZnO_{0.01}CuPc_{0.003}$	7.13	1.24	0.31	0.0054	26.76	1.34	1.39

Table 3. (2θ), d-spacing, FWHM and percentage intensity for ZnO-CuPc nanocomposite samples

Samples	(hkl)	(2θ) (°)	d (A°)	FWHM (°)	Intensity (%)
Pure $ZnO_{0.01}$	100	31.69	2.82	0.44	100
	002	34.56	2.59	0.41	21.04
	004	72.50	1.3	0.35	9.81
$ZnO_{0.01}CuPc_{0.001}$	100	7.42	12.03	0.36	36.93
	211	21.24	4.1	0.35	92.03
	100	31.69	2.82	0.31	45.18
$ZnO_{0.01}CuPc_{0.002}$	100	7.09	12.62	0.38	100
	102	9.26	9.62	0.39	76.99
	100	31.74	2.82	0.41	34.4
$ZnO_{0.01}CuPc_{0.003}$	100	7.13	1.24	0.31	100
	102	9.26	9.62	0.33	78.2
	002	31.69	2.82	0.34	50.8

3.2. FTIR Analysis

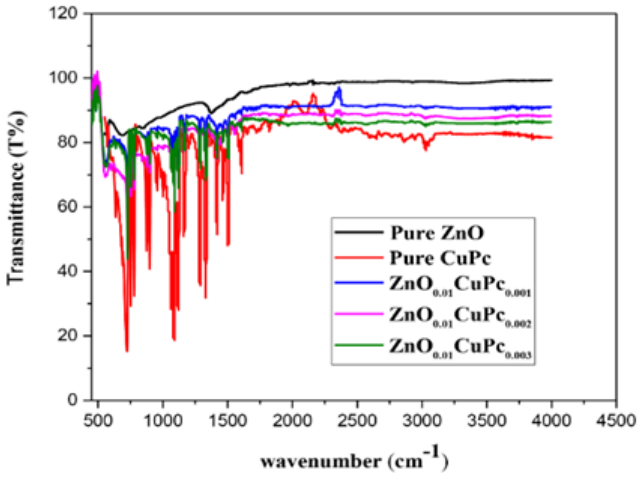

Figure 3. FTIR spectra for ZnO nanoparticles doped CuPc

The FTIR spectra for ZnO-CuPc nanocomposite has been recorded to study the various functional groups of nanocomposites displayed in Fig. 3. Infrared studies were carried out to ascertain the purity and nature of the metal nanoparticles. Metal oxides generally give absorption bands in the fingerprint region i.e. below 1000 cm^{-1} arising from inter-atomic vibrations. The peak observed at 1119.15 cm^{-1} may be due to O-H stretching and deformation, respectively assigned to the water adsorption on the metal surface. The characteristic wurtzite lattice vibrations (Zn-O) are corresponding to the broadband in range 400-600 cm^{-1} (Markova-Deneva 2010). The FTIR spectrum for CuPc, has characteristic peaks at 3040 cm^{-1} and 2930 cm^{-1} for aromatic C–H stretching, 1609 cm^{-1} for C=C macro cycle ring deformation,1504 cm^{-1} for C=N stretching, 1331 cm^{-1} for C–C stretching in is indole, 1090 cm^{-1} for C–H in plane deformation and 728 cm^{-1} for C–H out of plane deformation. The other peaks at 1290 cm^{-1}, 1161 $cm^{-1}$and 1119 cm^{-1} correspond to C–N stretching in indole, C-N enplane bending, C-H in plane bending, respectively (Singh et al. 2008).

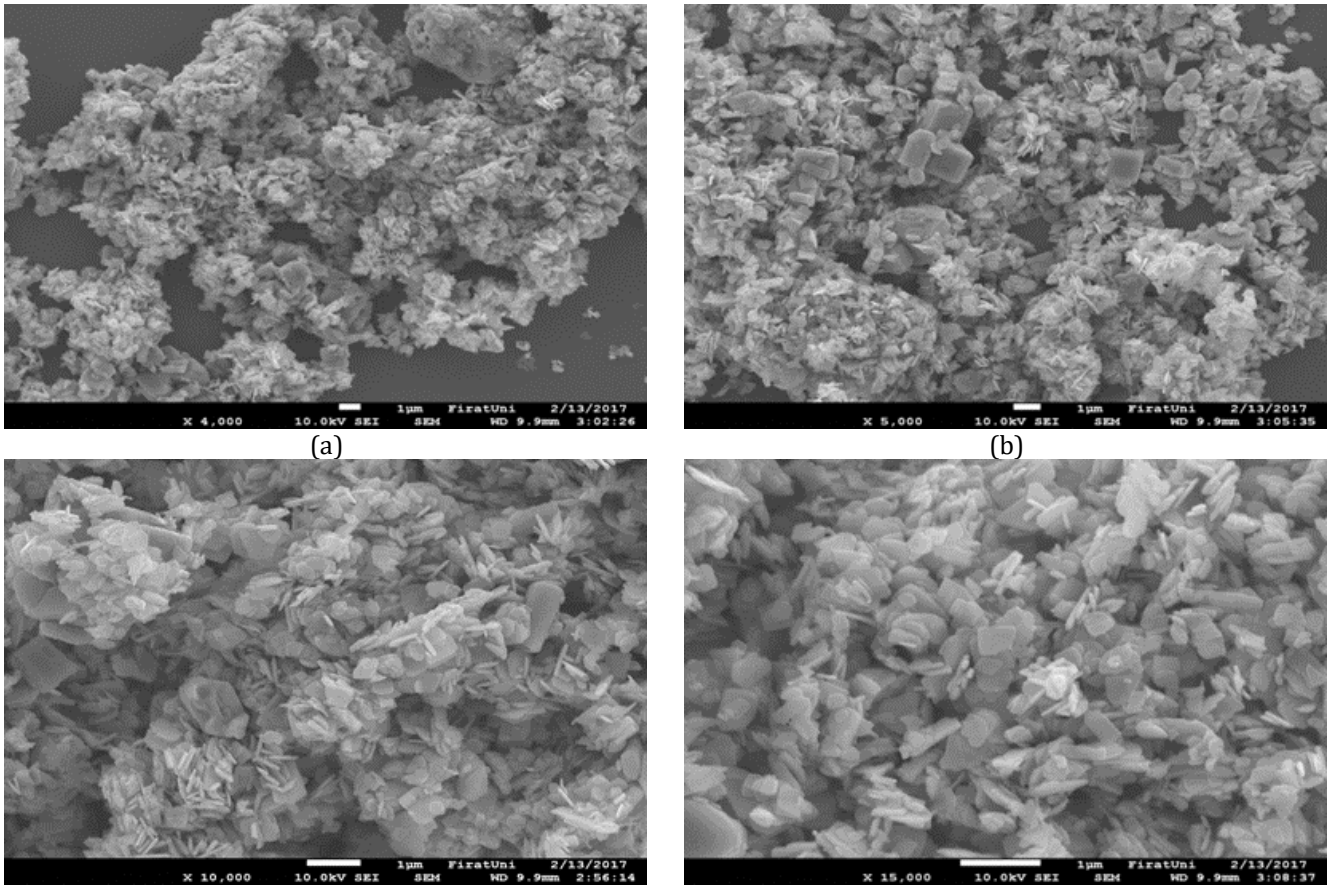

Figure 4. SEM micrograph for pure $ZnO_{0.01}$ (a) 4000x, (b) 5000x, (c) 10000x, (d) 15000x magnification

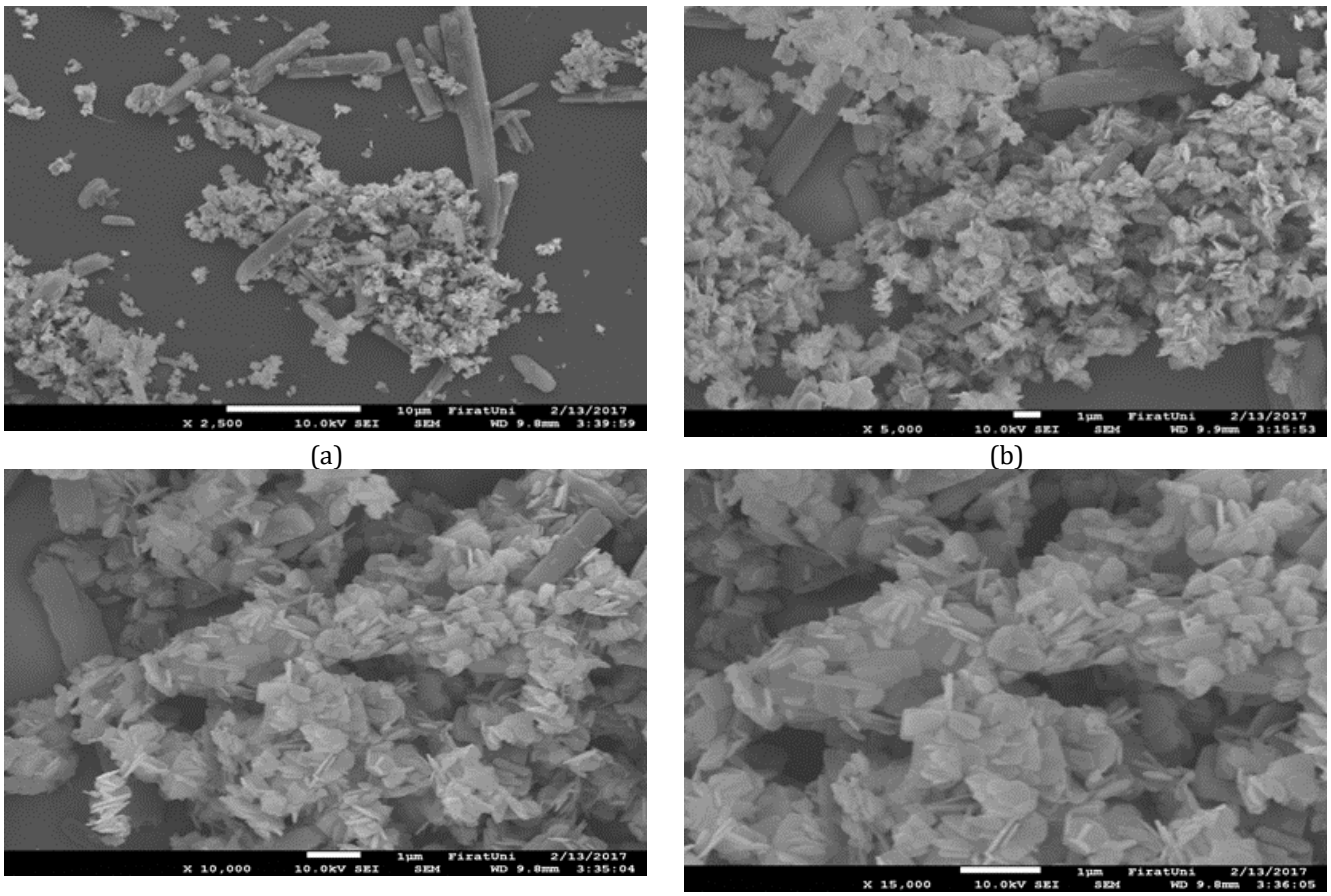

Figure 5. SEM micrograph for $ZnO_{0.01}$ $CuPc_{0.00101}$ (a) 4000x, (b) 5000x, (c) 10000x, (d) 15000x magnification

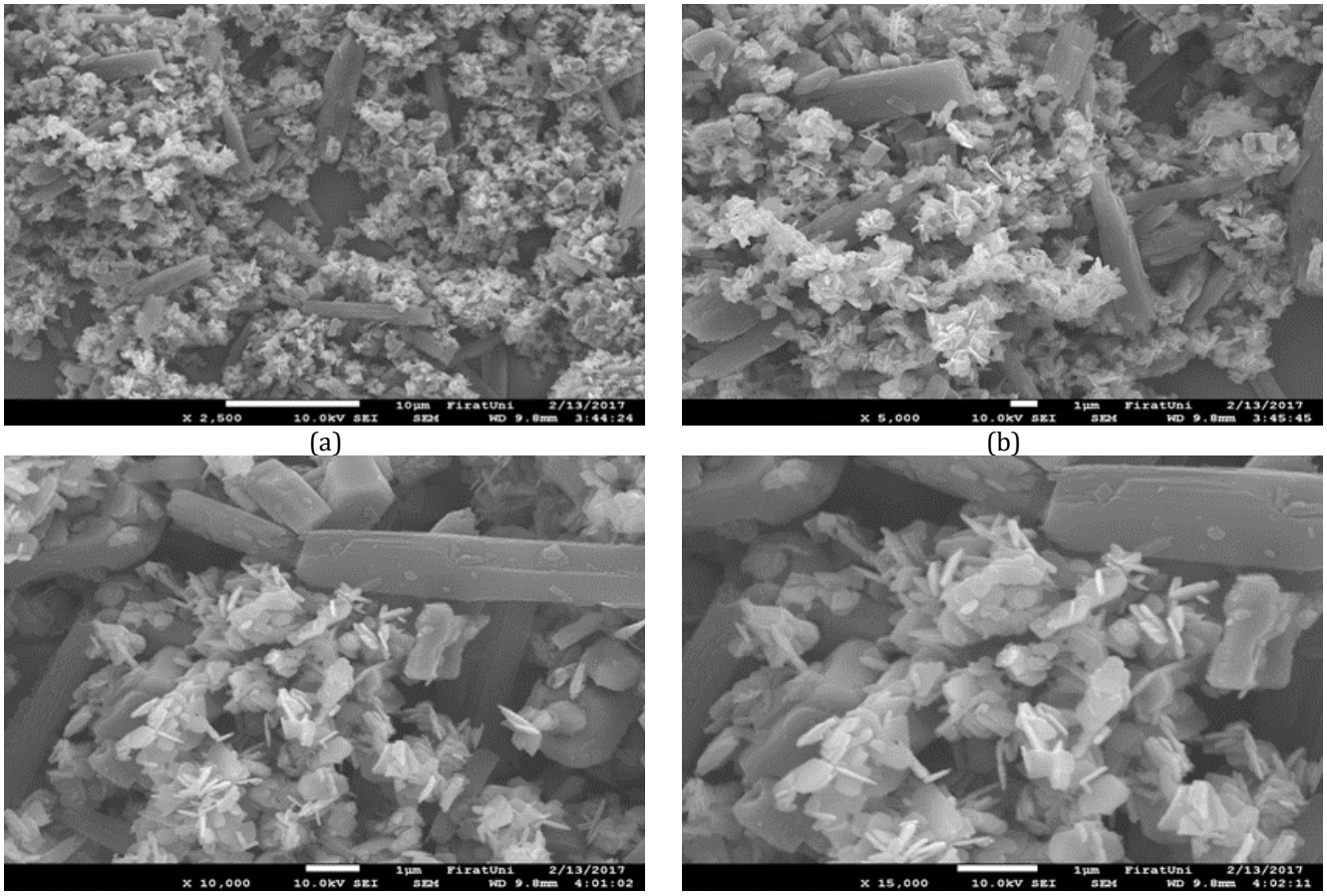

(a) (b)

(c) (d)

Figure 6. SEM micrograph for $ZnO_{0.01}$ $CuPc_{0.00201}$ (a) 4000x, (b) 5000x, (c) 10000x, (d) 15000x magnification

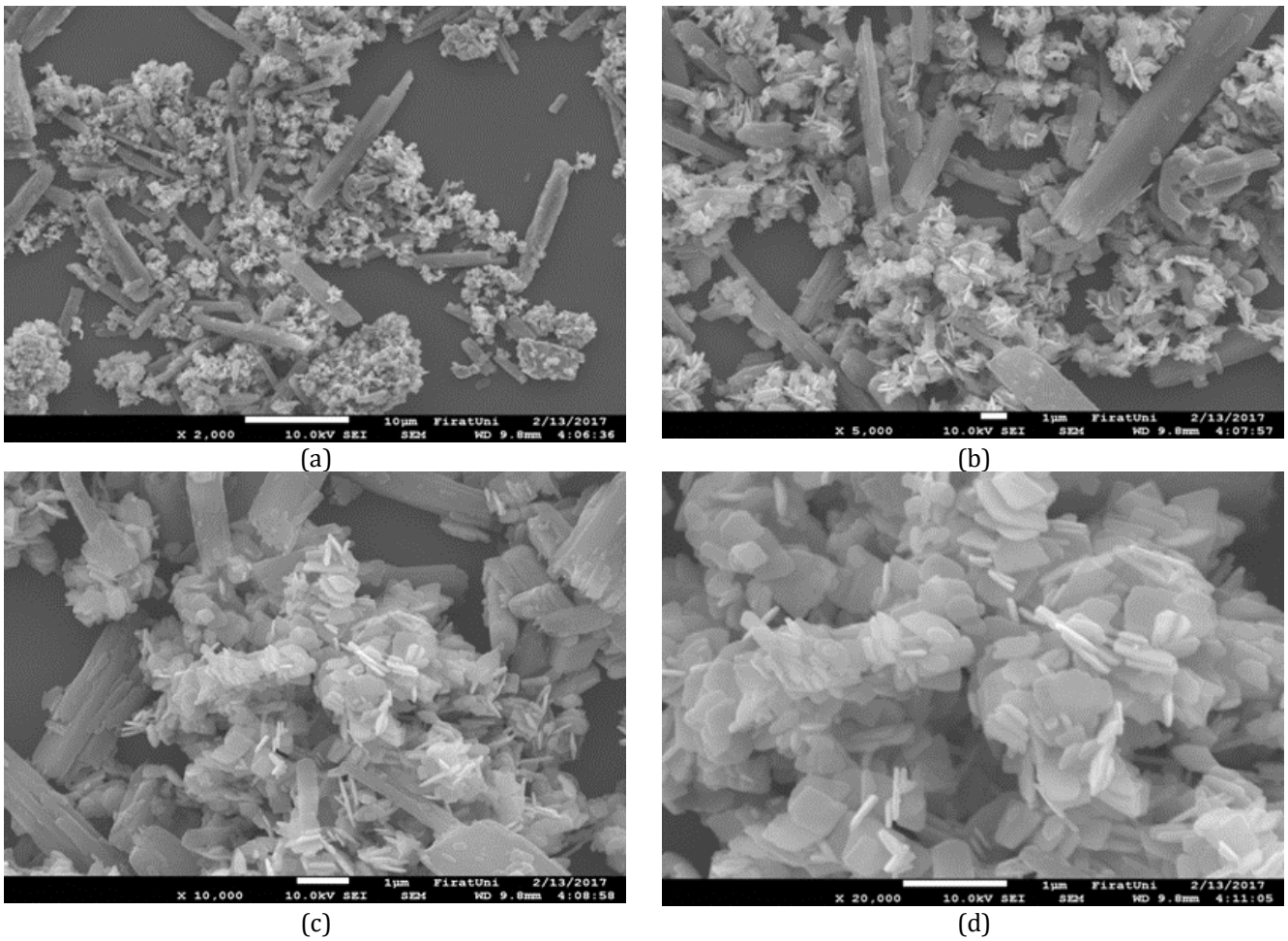

(a) (b)

(c) (d)

Figure 7. SEM micrograph for $ZnO_{0.01}$ $CuPc_{0.00301}$ (a) 4000x, (b) 5000x, (c) 10000x, (d) 15000x magnification

Table 4. EDX Analysis

	$ZnO_{0.01}$		$ZnO_{0.01}$ $CuPc_{0.001}$		$ZnO_{0.01}$ $CuPc_{0.002}$		$ZnO_{0.01}$ $CuPc_{0.003}$	
Element	Weight (%)	Atomic (%)	Weight (%)	Atomic (%)	Weight (%)	Atomic (%)	Weight (%)	Atomic (%)
CK	-	-	32.87	52.08	59.83	75.30	43.14	64.27
NK	-	-	8.05	11.89	13.45	14.51	9.15	11.69
OK	21.33	52.56	17.78	22.97	5.55	5.24	12.98	14.52
CuL	-	-	1.43	0.46	8.27	1.97	1.45	0.41
ZnL	78.67	47.44	39.87	12.61	12.91	2.99	33.28	9.11
Total	100.00	100.00	100.00	100.00	100.00	100.00	100.00	100.00

3.3. Morphological Analysis

In addition to automated SEM techniques, SEM morphological analysis fully characterized the materials. Though automated SEM analysis offers measured information about size, amount of phases and particles present and chemistry, the morphological analysis offers information about the physical relationships of the phases present, crystallinity and size.

The surface morphology of ZnO-CuPc nanocomposite was studied using FESEM at various magnifications and shown in Fig 4 (a,b,c,d). The pure ZnO, clearly shows (at 2500x, 5000x, 10000x, 15000x different magnifications) the formation of typical rod and clusters. In Fig. 5-7 (a,b,c,d) for ZnO-CuPc clearly shows (2500x, 5000x, 10000x, 15000x magnification) the formation of typical rod and clusters. The ESX spectrum of the samples are given in Table 4.

4. CONCLUSION

ZnO was synthesized by using the hydrothermal technique then doped with CuPc to make composites with different compositions. Characterization study was carried out using XRD, SEM and FTIR. The XRD patterns are used for phase identification and they showed the amount of impurities and structure depending on the peaks present in the samples. Diffraction pattern displays the hexagonal phase ZnO and for Cu-Pc have different crystal phases: α-, β- and χ– phases. XRD Scherer's formula is used to find the crystallite size of ZnO and doped with CuPc ($0.9\lambda/(B^*\cos\theta)$). SEM micrograph used to determine the microstructure and typically rod and clusters formations were observed. FTIR spectra have been recorded to several functional groups.

ACKNOWLEDMENT

This work is financially supported by FÜBAP, Project No: FF.16.33.

REFERENCES

Güler Ö, Güler S H, Başgöz Ö, Albayrak M G & Yahia I S (2019). Synthesis and characterization of ZnO-reinforced with graphene nanolayer nanocomposites: electrical conductivity and optical band gap analysis. Materials Research Express, 6(9), 095602. DOI: 10.1088/2053-1591/ab2b12

Güler S H, Güler Ö, Evin E & Islak S (2016). Electrical and optical properties of ZnO-milled Fe_2O_3 nanocomposites produced by powder metallurgy route. Optik, 127(6), pp. 3187-3191. DOI: 10.1016/j.ijleo.2015.12.103

Heilmeier G H & Warfield G (1963). Photoconductivity in Metal-Free Phthalocyanine Single Crystals. The Journal of Chemical Physics, 38(4), 897-901. DOI: 10.1063/1.1733780

Hussein M T, Aadim K A & Hassan E K (2016). Structural and surface morphology analysis of copper phthalocyanine thin film prepared by pulsed laser deposition and thermal evaporation techniques. Advances in Materials Physics and Chemistry, 6(4), 85-97. DOI: 10.4236/ampc.2016.64009

Kahraman S, Çetinkaya S, Yaşar S & Bilican İ (2014). Polyethylene glycol-assisted growth of Cu_2SnS_3 promising absorbers for thin film solar cell applications. Philosophical Magazine, 94(27), 3149-3161. DOI: 10.1080/14786435.2014.952257

Khan Z R, Zulfequar M & Khan M S (2010). Optical and structural properties of thermally evaporated cadmium sulphide thin films on silicon (1 0 0) wafers. Materials Science and Engineering: B, 174, (1-3), 145-149. DOI: 10.1016/j.mseb.2010.03.006

Markova-Deneva I (2010). Infrared spectroscopy investigation of metallic nanoparticles based on copper, cobalt, and nickel synthesized through borohydride reduction method. Journal of the University of Chemical Technology and Metallurgy, 45(4), 351-378.

Saleem M, Fang L, Ruan H B, Wu F, Huang Q L, Xu C L & Kong C Y (2012). Effect of zinc acetate concentration on the structural and optical properties of ZnO thin films deposited by Sol-Gel method. International Journal of Physical Sciences, 7(23), 2971-2979. DOI: 10.5897/IJPS12.219

Scherrer P (1918). Bestimmung dergrosse und der inneren struktur yon kolloiteilchen mittels. Gottinger Nachr Math Phys, 2, 98-100. (in Deutsch)

Singh S, Tripathi S K & Saini G S S (2008). Optical and infrared spectroscopic studies of chemical sensing by copper phthalocyanine thin films. Materials Chemistry and Physics, 112(3), 793-797. DOI: 10.1016/j.matchemphys.2008.06.044

Xavier F P (1997). Application of electroreflectance analysis for organic semiconductor thin films. Bulletin of Materials Science, 20(5), 651-665.